Dispersion of the electron g factor anisotropy in InAs/InP self-assembled quantum dots

Dispersion of the electron *g* factor anisotropy in InAs/InP self-assembled quantum dots

V. V. Belykh,[1,2,a)] D. R. Yakovlev,[1,3] J. J. Schindler,[1] J. van Bree,[4] P. M. Koenraad,[4] N. S. Averkiev,[3] M. Bayer,[1,3] and A. Yu. Silov[4,b)]
[1]*Experimentelle Physik 2, Technische Universität Dortmund, D-44221 Dortmund, Germany*
[2]*P.N. Lebedev Physical Institute of the Russian Academy of Sciences, Moscow 119991, Russia*
[3]*Ioffe Institute, Russian Academy of Sciences, 194021 St. Petersburg, Russia*
[4]*Department of Applied Physics and COBRA Research Institute, Eindhoven University of Technology, P.O. Box 513, 5600 MB Eindhoven, The Netherlands*

(Received 4 June 2016; accepted 5 August 2016; published online 22 August 2016)

The electron *g* factor in an ensemble of InAs/InP quantum dots with emission wavelengths around 1.4 μm is measured using time-resolved pump-probe Faraday rotation spectroscopy in different magnetic field orientations. Thereby, we can extend recent single dot photoluminescence measurements significantly towards lower optical transition energies through 0.86 eV. This allows us to obtain detailed insight into the dispersion of the recently discovered *g* factor anisotropy in these infrared emitting quantum dots. We find with decreasing transition energy over a range of 50 meV a strong enhancement of the *g* factor difference between magnetic field normal and along the dot growth axis, namely, from 1 to 1.7. We argue that the *g* factor cannot be solely determined by the confinement energy, but the dot asymmetry underlying this anisotropy therefore has to increase with increasing dot size. *Published by AIP Publishing*. [http://dx.doi.org/10.1063/1.4961201]

I. INTRODUCTION

Semiconductor quantum dots (QDs) provide an attractive platform for manipulating electron and hole spins both for practical applications and fundamental research.[1] In this respect, the main advantage of QDs over systems of higher dimensionality is the long spin coherence time[2] owing to the suppressed spin-orbit interaction.[3] The other advantage of QDs is the possibility to tune carrier *g* factors which determine the susceptibility of the spin to a magnetic field and, correspondingly, spin-spin interactions. The electron *g* factor depends on the details of QD confinement and is significantly different from the one in a corresponding bulk semiconductor,[4–6] especially for strong confinement.[7] In particular, any QD anisotropy translates into an anisotropy of the *g* factors.[8,9]

A carrier *g* factor characterizes its magnetic moment and has contributions from both spin and orbital degrees of freedom. For a free electron (or a bound electron in the ground state), only the spin moment contributes to the total magnetic moment so that $g \approx +2$. However, it is well known that the *g* factor of materials with spin-orbit coupling is significantly modified due to spin-correlated orbital currents.[10,11] The spatial structure of these currents has been recently studied for a ground state electron confined in a nanostructure.[12] These currents were found to form effectively a current loop perpendicular to the magnetic moment's orientation[9] and, therefore, represent an orbital moment $\mu_{\mathrm{orb}} = IA$ (here, I is the integrated current and A is the area the current encircles). This spin-dependent orbital moment causes the deviation of the ground state electron *g* factor from the free electron value of +2. The orbital moment decreases monotonically with decreasing size[12,13] due to the interplay of the separate size-dependencies of I and A.

There are two widely used ways to determine electron *g* factors: The *g* factor averaged over a QD ensemble can be determined in a pump-probe Faraday rotation experiment from the Larmor frequency ω_{L} of the spin precession about an external magnetic field B: $\hbar\omega_{\mathrm{L}} = |g|\mu_{\mathrm{B}}B$.[7,8,14–18] Alternatively, the *g* factor can be determined also from the Zeeman splitting of the emission lines in single QD photoluminescence (PL).[9,19] In both cases, the field orientation can be varied, giving access to the *g*-factor tensor components.

Electron *g* factors have been extensively studied for QDs with emission wavelengths shorter than 1 μm (above 1.25 eV optical transition energy). *A priori* one might assume that the electron *g* factor is roughly spatially isotropic. Only recently corresponding studies for QDs emitting in the telecom wavelength range were reported.[8,9] Surprisingly, the electron *g* factor shows a strong anisotropy in these systems. For InAs/InP QDs, single dot PL revealed a difference of about unity for the electron *g* factors normal and along the growth axis, $g_{\perp} - g_{\parallel} \sim 1$, having even opposite signs in the energy range from 0.9 to 1.0 eV.[9] However, the single QD PL spectroscopy did not provide any means of measuring the individual values of $g_{\parallel}$ over a wide range of energies below 0.9 eV in this system, where it was impossible to separate the hole and electron contributions, see Ref. 9 for details. Also, for InAs/InAlGaAs QDs, a similar difference of unity was observed in the energy range from 0.77 to 0.84 eV, however, with both being negative.[8] Knowledge of the origin and magnitude of this anisotropy are essential if one wants to use spins confined in such structures for intermediary information storage in communication technology. Manipulation of the spins by microwaves requires then adjustment of the radiation frequency when changing the magnetic field direction.

a)vasilii.belykh@tu-dortmund.de
b)A.Y.Silov@tue.nl

In the present work, we study electron g factors in InAs QD ensembles embedded in InP barriers, emitting at about $\sim$1.4 μm wavelength, using pump-probe Faraday rotation measurements for different orientations of the magnetic field. The strong confinement of the studied QDs leads to a strong g-factor anisotropy $\delta g_e = g_{e\perp} - g_{e||}$ between the transverse $g_{e\perp}$ (**B** perpendicular to the growth axis z) and the longitudinal $g_{e||}$ (**B** parallel to that axis), which drastically increases with decreasing transition energy.

An important aspect of our studies is the possibility to compare the g factors determined here with those measured by single QD PL spectroscopy on the same structures in the range of higher energies.[9] The dephasing time T_2^* of the signal in Faraday rotation is typically attributed to the variation of the g factor in the ensemble according to $1/T_2^* = \Delta g \mu_B B/\hbar$. The resulting spread is in good accord with the g factor variation observed in single QD PL.

II. EXPERIMENTAL DETAILS

The sample under study was grown by metal-organic vapor phase epitaxy (MOVPE). A 100 nm InP layer was deposited on an n-doped InP (100) substrate with a 2° miscut toward the (110) direction. Two monolayers of GaAs were deposited as an interlayer on top of which two InAs monolayers are grown, resulting in the formation of QDs. The quantum dot layer was capped by 200 nm of InP. More details about the growth of such QDs can be found in Ref. 20. A PL spectrum of the QD ensemble taken at temperature $T = 4.5$ K is shown in Fig. 1(a). The emission is centered around 0.9 eV and has a large inhomogeneous broadening originating from the spread of QD parameters. The multiple peak structure is attributed to the multimodal height distribution of the QDs.[21]

The sample was installed in a vector magnet system consisting of three superconducting split-coils oriented orthogonally to each other. By adjusting the current in each coil, both the magnitude (up to 3 T) and the direction of the magnetic field B can be varied, while keeping the sample position unchanged relative to the optical axis. The sample was in contact with helium gas at a temperature $T \approx 15$ K.

A time-resolved pump-probe technique with polarization sensitivity was applied to measure the electron spin dynamics. We used a NT&C laser system consisting of an Optical Parametric Amplifier (OPA) pumped by a mode-locked Yb:KGW laser operating at 1040 nm.[22] The system generates a periodic train (repetition rate 40 MHz) of 300-fs-long pulses with the center wavelength tunable in the range of 1350–4500 nm. By means of a pulse shaper, the broadband spectrum ($\sim$50 nm) is shaped to a width of 20 nm (10 meV) centered at the desired wavelength. The laser output is split into a pump and a probe beam. The circularly polarized pump generates the carrier spin polarization, which is probed by measuring the ellipticity (the difference in the intensities of the beam components with σ^+ and σ^- helicities) of the initially linearly polarized probe beam after transmission through the sample. The temporal evolution of the carrier spin polarization is traced by varying the delay between the pump and probe. This method is analogous to measuring the Faraday rotation of the probe beam and provides similar information.[18] The polarization of the pump beam was modulated between σ^+ and σ^- by a photo-elastic modulator operated at a frequency of 84 kHz to perform a synchronous detection scheme and to avoid polarization of nuclei. The experimental geometry is shown in Fig. 1(b).

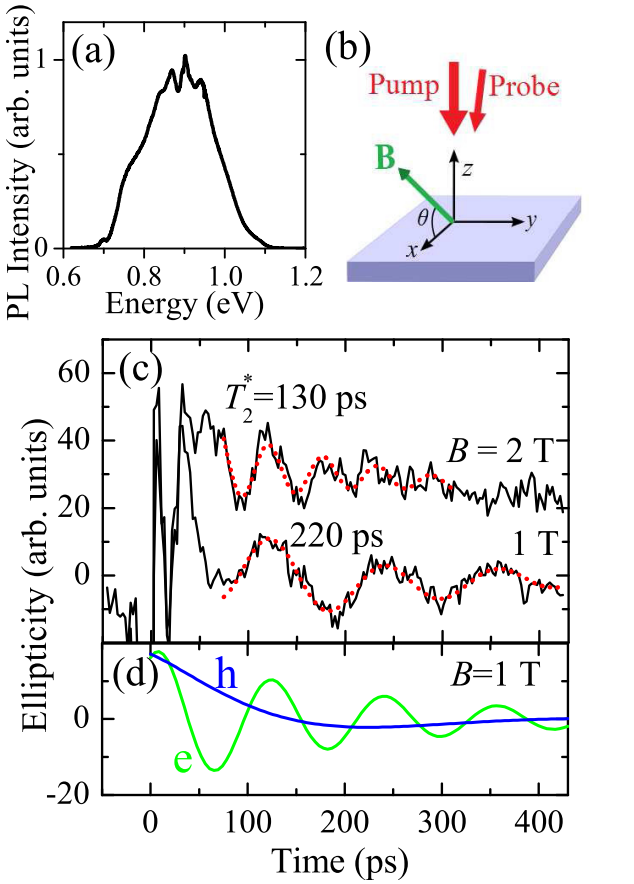

FIG. 1. (a) Photoluminescence spectrum of the studied InAs/InP QDs at $T = 4.5$ K. (b) The experimental geometry. (c) Dynamics of the ellipticity signal from the studied QDs at different magnetic fields. The curves are shifted vertically for clarity. Red dotted lines show fits to the experimental data. The fit form is given by the sum of two damped oscillating functions. (d) Electron and hole contributions extracted from the fit to the dynamics at $B = 1$ T. The laser photon energy is set to 0.91 eV, and the magnetic field is applied in Voigt geometry.

III. RESULTS AND DISCUSSION

The dynamics of the ellipticity signal for the magnetic field applied in Voigt geometry (perpendicular to the pump and probe beams as well as the sample growth axis) shows pronounced oscillations resulting from the electron spin Larmor precession (see Fig. 1(c)). The signals are fitted by the sum of two damped oscillating functions of the form $\cos(\omega_L t)\exp(-t/T_2^*)$, where t is the delay time, ω_L is the precession frequency, and T_2^* is the spin dephasing time.[8] The fit gives an oscillating component with a frequency proportional to B, corresponding to a g-factor modulus of 0.6. Single QD PL experiments[9] allow one to attribute this g factor at 0.91 eV optical transition energy to the electrons and to assign a positive sign to the g factor: $g_{e\perp} \approx +0.6$. Note that exciton effects, i.e., the exchange interaction of electron and hole, would lead to an offset in the dependence of the

oscillation frequency on B,[15] which in our case is negligibly small. The fit also gives a slowly oscillating component with an oscillation frequency corresponding to $|g| \approx 0.1$. We attribute it to the hole spin precession, in agreement with single QD measurements. Since the corresponding oscillation period is comparable to the signal decay time, a precise evaluation of this g factor is impossible, and in the following, we do no longer consider the hole spins. The two contributions to the dynamics obtained from the best fit of the experimental data at $B = 1$ T are shown in Fig. 1(d). The electron spin dephasing time T_2^* of about 220 ps is shorter than the exciton recombination time of ~1 ns and is related to the spread Δg of the g factor within the studied QD ensemble:[8] $1/T_2^* = \Delta g \mu_B B/\hbar$. Indeed, T_2^* decreases from 220 ps down to 130 ps with a field increase from 1 to 2 T, which corresponds to $\Delta g_{e\perp} \approx 0.06$.

To determine the longitudinal g factors, $g_{e||}$, we measured the ellipticity dynamics with the magnetic field **B** tilted relative to the sample plane xy by a finite angle θ. An increase of θ leads to a decrease of the oscillation amplitude, as described in Refs. 8 and 23. The oscillations can be reliably resolved for $\theta \lesssim 30°$. The angular dependence of the electron g-factor modulus for different laser energies is presented in Fig. 2. Interestingly, the dependence at 0.91 eV is rather weak, varying only slightly from 0.6 up to 0.7, while the changes become much larger at the low energies so far not studied for these QDs: in particular, at 0.86 eV, the electron g-factor varies from 0.3 up to 0.8. Note again that pump-probe Faraday rotation allows one to measure only the absolute value of the g factor $|g_e|$ and not the sign of the g factor. Therefore, we take over the sign assignment from the single QD PL experiments reported in Ref. 9. There it was shown that $g_{e\perp} > 0$ and $g_{e||} < 0$.

For an anisotropic g factor, the Larmor precession vector $\boldsymbol{\omega}_L$ is not necessarily collinear with the external magnetic field **B** that causes the spin precession.[8] Using the principal

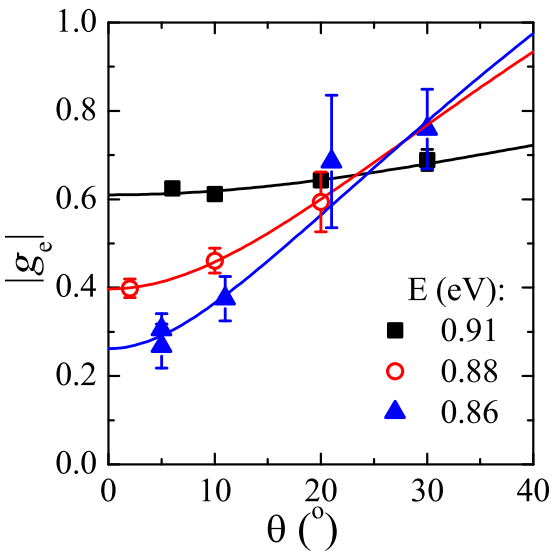

FIG. 2. Dependence of the electron g-factor modulus on the angle between the sample surface and the magnetic field for different optical transition energies. Zero angle corresponds to the Voigt geometry. Solid lines show fits to the experimental data with Eq. (2).

axes of the g factor tensor, the angle α between $\boldsymbol{\omega}_L$ and **B** is given by

$$\cos\alpha = \frac{g_\perp (B\cos\theta)^2 + g_\parallel (B\sin\theta)^2}{B\sqrt{(g_\perp B\cos\theta)^2 + (g_\parallel B\sin\theta)^2}}, \quad (1)$$

where the magnetic field is tilted by an angle θ with respect to the sample plane. Also, we assume that the transverse g factor ($g_\perp$) shows no anisotropy, that is, $g_{[011]} = g_{[0\bar{1}1]}$. It is easily seen from Eq. (1) that the spin angular momentum precesses about the magnetic field only if either the in-plane component of the field, $B_\perp = B\cos\theta$, or its out-of-plane projection, $B_\parallel = B\sin\theta$, is zero. For all other field orientations, this is, however, not the case. To give a particular example, when $g_\perp = -g_\parallel$ and the magnetic field is tilted by 45°, the vector of Larmor precession is perpendicular to the magnetic field, whereas the precession frequency remains unchanged with angle variation. In general, the Larmor frequency in tilted field is given by

$$\omega_L(\theta) = \frac{\mu_B B}{\hbar}\sqrt{(g_\perp\cos\theta)^2 + (g_\parallel\sin\theta)^2}. \quad (2)$$

Note that it is impossible to analyze any sign anisotropy of the g factor by measuring the angular dependence of the Larmor frequency $\omega_L(\theta)$, as it is not sensitive to a change in sign of the g-factor tensor components. Figure 3 illustrates this point further.

The experimental dependencies for $g_e(\theta)$ (the symbols in Fig. 2) were fitted by Eq. (2) (the solid lines), from which the absolute values of the transverse and longitudinal electron g factors were evaluated. By applying the magnetic field along different directions in the sample plane, we also confirmed that the in-plane anisotropy of the g factor is negligible, i.e., $g_{[011]} = g_{[0\bar{1}1]}$.

The energy dependencies of $g_{e\perp}$ and $g_{e||}$, determined from the pump-probe ellipticity measurements, are shown by the solid symbols in Fig. 4. For comparison, we included the $g_{e\perp}$ and $g_{e||}$ as previously determined[9] from the Zeeman splitting of the single dot emission lines in PL spectra (the open symbols).

From these plots, we find three prominent observations. First, we observe in Fig. 4 for both types of measurements that $g_{e\perp}$ and $g_{e||}$ increase with optical transition energy. This agrees well with the findings based on the spin-correlated orbital currents:[12,13] Previous structural characterization of these InAs/InP QDs revealed that their shape resembles approximately flat disks.[4] The dots have fixed InAs composition with negligible intermixing with the barriers, so that the variation of QD emission energies is almost completely related to variation of the dot size. Therefore, also the variation of the electron g factors is closely correlated with the dot size. An increase of the emission energy corresponds to a decreasing of QD size and therefore leads to a smaller spin-correlated orbital moment. Hence, the g factor tends to +2.

Second, we consistently measure $g_{e\perp} > g_{e||}$, as was also reported for the electron g factor in other QDs.[8] The picture of the loop formed by the spin-correlated current provides a simple explanation for this finding. Due to the disk shape of

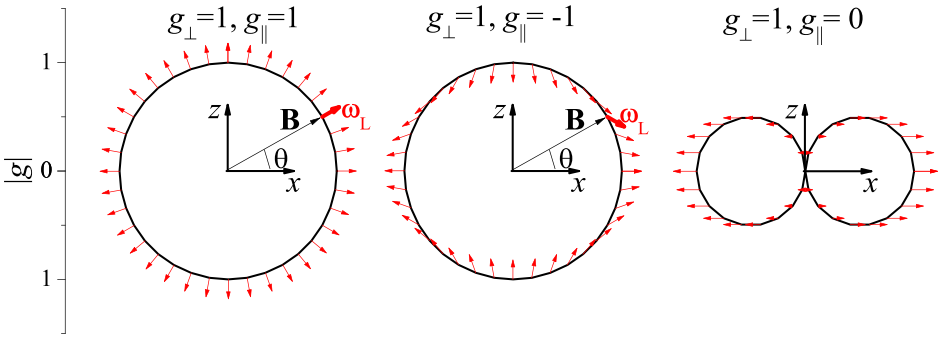

FIG. 3. Larmor precession vector $\boldsymbol{\omega}_L$ (arrows) and modulus of the g factor (solid lines) versus the tilt angle θ of the magnetic field **B**. From left to right, three different examples of g-tensor anisotropies are illustrated.

the QDs, the spin-correlated orbital currents can encircle a larger area when the moment is oriented along the z-axis than when it is oriented along the x-axis.[9] This results in $\mu_{\mathrm{orb},x} < \mu_{\mathrm{orb},z}$, which translates into $g_{e\perp} > g_{e\parallel}$.

Third, we observe that the $g_{e\perp}$ values measured on individual QDs in PL show a scattering that coincides with the $\Delta g_{e\perp}$ determined from the spin dephasing time in the pump-probe experiments (the shaded area in Fig. 4). This gives a nice confirmation of the correlation between spin dephasing time and the g-factor spread in the QD ensemble. For high transition energies, the spread of $\Delta g_{e\perp}$ is small, while for decreasing energies, both spreads become larger. This is somewhat surprising as a larger dot size typically leads to a weaker sensitivity of electronic properties to this size. The larger spread indicates that in the low emission energy range QDs with different heights contribute to the emission, leading to considerable change of the area of the spin-correlated current.

We point out that the electron g factors obtained for these InAs/InP QDs are closer to +2 than those obtained for InAs/$In_{0.53}Al_{0.24}Ga_{0.23}As$ QDs, even though they emit in a similar spectral range[8] (e.g., $g_{e\perp} = -1.5$ and $g_{e\parallel} = -2.4$ at 0.84 eV). This difference can be attributed to both different size and composition. The InAs/$In_{0.53}Al_{0.24}Ga_{0.23}As$ QDs have a larger average size so that the orbital currents can generate a larger orbital moment. This results in g factors showing a stronger deviation from +2. Also, the difference in composition affects the orbital moment: the amount of current that is circulating depends on the material parameters. Therefore, the g factor in QDs is not solely determined by their emission (or confinement) energy.

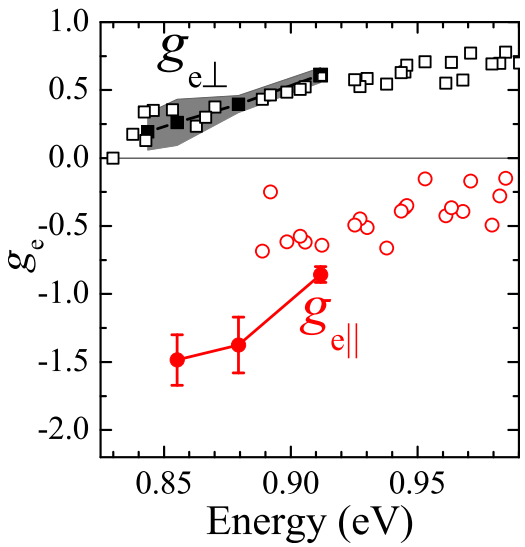

FIG. 4. Dependence of the electron g-factor components on optical transition energy. Solid and open symbols show the g factors determined from pump-probe ellipticity (this work) and single dot PL (from Ref. 9), respectively. Squares and circles show transverse and longitudinal g factors, respectively. The shaded area shows the spread of the transverse g factor determined from the spin dephasing time. Solid lines are guides to the eye.

IV. CONCLUSIONS

In conclusion, we have studied the electron spin dynamics in InAs/InP QDs emitting around 1.4 μm in magnetic fields of different orientations. The average electron g factor in a QD ensemble was measured in that way. At optical transition energies of about 0.86 eV (not addressed so far in single dot PL studies), the electron g factor shows a considerable anisotropy with $g_{e\perp} \approx 0.3$ and $g_{e\parallel} \approx -1.5$. Further studies on different QDs are desirable to explore the potential of these structures for tailoring the carrier g factors on a detailed level.

ACKNOWLEDGMENTS

We are grateful to A. Greilich, E. L. Ivchenko, and E. A. Zhukov for valuable advices and useful discussions. We acknowledge the financial support from the Russian Science Foundation (Grant No. 14-42-00015) and the Deutsche Forschungsgemeinschaft in the frame of the ICRC TRR 160.

[1]F. Henneberger and O. Benson, *Semiconductor Quantum Bits* (Pan Stanford, 2008).
[2]A. Greilich, D. R. Yakovlev, A. Shabaev, A. L. Efros, I. A. Yugova, R. Oulton, V. Stavarache, D. Reuter, A. Wieck, and M. Bayer, Science **313**, 341 (2006).
[3]A. V. Khaetskii and Y. V. Nazarov, Phys. Rev. B **61**, 12639 (2000).
[4]J. van Bree, A. Yu. Silov, P. M. Koenraad, M. E. Flatté, and C. E. Pryor, Phys. Rev. B **85**, 165323 (2012).
[5]A. A. Kiselev, E. L. Ivchenko, and U. Rössler, Phys. Rev. B **58**, 16353 (1998).
[6]E. Ivchenko and A. Kiselev, Sov. Phys. Semicond. **26**, 827 (1992).
[7]V. V. Belykh, A. Greilich, D. R. Yakovlev, M. Yacob, J. P. Reithmaier, M. Benyoucef, and M. Bayer, Phys. Rev. B **92**, 165307 (2015).
[8]V. V. Belykh, D. R. Yakovlev, J. J. Schindler, E. A. Zhukov, M. A. Semina, M. Yacob, J. P. Reithmaier, M. Benyoucef, and M. Bayer, Phys. Rev. B **93**, 125302 (2016).
[9]J. van Bree, A. Yu. Silov, M. L. van Maasakkers, C. E. Pryor, M. E. Flatté, and P. M. Koenraad, Phys. Rev. B **93**, 035311 (2016).
[10]L. M. Roth, B. Lax, and S. Zwerdling, Phys. Rev. **114**, 90 (1959).
[11]Y. Yafet, Solid State Phys. **14**, 1 (1963).

[12]J. van Bree, A. Yu. Silov, P. M. Koenraad, and M. E. Flatté, Phys. Rev. Lett. **112**, 187201 (2014).
[13]J. van Bree, A. Yu. Silov, P. M. Koenraad, and M. E. Flatté, Phys. Rev. B **90**, 165306 (2014).
[14]A. Greilich, R. Oulton, E. A. Zhukov, I. A. Yugova, D. R. Yakovlev, M. Bayer, A. Shabaev, A. L. Efros, I. A. Merkulov, V. Stavarache, D. Reuter, and A. Wieck, Phys. Rev. Lett. **96**, 227401 (2006).
[15]I. A. Yugova, A. Greilich, E. A. Zhukov, D. R. Yakovlev, M. Bayer, D. Reuter, and A. D. Wieck, Phys. Rev. B **75**, 195325 (2007).
[16]M. V. G. Dutt, J. Cheng, B. Li, X. Xu, X. Li, P. R. Berman, D. G. Steel, A. S. Bracker, D. Gammon, S. E. Economou, R.-B. Liu, and L. J. Sham, Phys. Rev. Lett. **94**, 227403 (2005).
[17]A. Schwan, B.-M. Meiners, A. Greilich, D. R. Yakovlev, M. Bayer, A. D. B. Maia, A. A. Quivy, and A. B. Henriques, Appl. Phys. Lett. **99**, 221914 (2011).
[18]M. M. Glazov, I. A. Yugova, S. Spatzek, A. Schwan, S. Varwig, D. R. Yakovlev, D. Reuter, A. D. Wieck, and M. Bayer, Phys. Rev. B **82**, 155325 (2010).
[19]M. Bayer, G. Ortner, O. Stern, A. Kuther, A. A. Gorbunov, A. Forchel, P. Hawrylak, S. Fafard, K. Hinzer, T. L. Reinecke, S. N. Walck, J. P. Reithmaier, F. Klopf, and F. Schäfer, Phys. Rev. B **65**, 195315 (2002).
[20]S. Anantathanasarn, R. Nötzel, P. J. van Veldhoven, T. J. Eijkemans, and J. H. Wolter, J. Appl. Phys. **98**, 013503 (2005).
[21]N. A. J. M. Kleemans, J. van Bree, M. Bozkurt, P. J. van Veldhoven, P. A. Nouwens, R. Nötzel, A. Yu. Silov, P. M. Koenraad, and M. E. Flatté, Phys. Rev. B **79**, 045311 (2009).
[22]J. Krauth, A. Steinmann, R. Hegenbarth, M. Conforti, and H. Giessen, Opt. Express **21**, 11516 (2013).
[23]G. Salis, D. D. Awschalom, Y. Ohno, and H. Ohno, Phys. Rev. B **64**, 195304 (2001).